Published in final edited form as:
Radiol Med. 2014 July ; 119(7): 521–532. doi:10.1007/s11547-014-0429-5.

C-arm cone-beam computed tomography in interventional oncology: technical aspects and clinical applications

Chiara Floridi,
Radiology Department, Insubria University, Viale Borri 57, 21100 Varese, Italy

Alessandro Radaelli,
Philips Healthcare, Woerden, The Netherlands

Nadine Abi-Jaoudeh,
Center for Interventional Oncology, National Institutes of, Health, Radiology and Imaging Sciences, Bethesda, USA

Micheal Grass,
Philips Research North America, Briarcliff Manor, USA

Philips Research, Hamburg, Germany

Ming De Lin,
Philips Research North America, Briarcliff Manor, USA

Philips Research, Hamburg, Germany

Melanie Chiaradia,
Department of Radiology and Medical Imaging, Henri Mondor, Hospital, Créteil, France

Jean-Francois Geschwind,
Division of Vascular and Interventional Radiology, Johns, Hopkins Hospital, Baltimore, USA

Hishman Kobeiter,
Department of Radiology and Medical Imaging, Henri Mondor, Hospital, Creteil, France

Ettore Squillaci,
Department of Diagnostic and Molecular Imaging, Interventional Radiology and Radiotherapy, University Tor, Vergata, Rome, Italy

Geert Maleux,
Department of Radiology, Leuven University Hospitals, Louvain, Belgium

Andrea Giovagnoni,
Department of Radiology, University of Ancona, Ancona, Italy

Luca Brunese,
Department of Radiology, University of Molise, Campobasso, Italy

chiara.floridi@gmail.com.

Conflict of interest The authors declare no conflict of interest.

Bradford Wood,
Center for Interventional Oncology, National Institutes of, Health, Radiology and Imaging Sciences, Bethesda, USA

Gianpaolo Carrafiello, and
Radiology Department, Insubria University, Viale Borri 57, 21100 Varese, Italy

Antonio Rotondo
Department of Radiology, Seconda Universita degli Studi, Naples, Italy

Abstract

C-arm cone-beam computed tomography (CBCT) is a new imaging technology integrated in modern angiographic systems. Due to its ability to obtain cross-sectional imaging and the possibility to use dedicated planning and navigation software, it provides an informed platform for interventional oncology procedures. In this paper, we highlight the technical aspects and clinical applications of CBCT imaging and navigation in the most common loco-regional oncological treatments.

Keywords

Interventional oncology; Cone-beam computed tomography; Imaging guidance; Percutaneous treatments; Embolization; Ablation

Introduction

Interventional oncology is a growing field offering new minimally invasive, image-guided treatment options for a variety of primary and metastatic solid tumors. Imaging is at the core of this approach and selection of the optimal diagnostic and interventional modalities is critical for a safe and effective treatment delivery [1]. Treatment options commonly involve either a selective intra-arterial administration of cytotoxic drugs or radioactive microspheres combined with blood-depriving embolic agents (embolo-therapy), or thermal destruction via a percutaneously inserted ablation device [2].

Two-dimensional (2D) angiography is the main imaging technique during embolotherapy. However, its intrinsic 2D nature and low-contrast resolution may render tumor and feeding arteries visibility challenging. Multiple angiograms in different views are required with subsequent increase in radiation exposure and procedural time or decrease in accuracy of intended selective delivery. Hybrid angiographic systems combined with computed tomography (CT) or magnetic resonance imaging (MRI) scanners have been used to bridge the gap between diagnostic and interventional imaging. These options offer excellent intra-procedural soft-tissue, MRI [3], and tumor and vascular depiction, CT [4] but associated costs and workflow considerations have limited their widespread adoption.

The most widely used imaging modalities to guide percutaneous tumor ablation are ultrasound and conventional CT. Ultrasound offers a versatile imaging technology for liver and kidney tumor ablation with real-time imaging. However, tumor and needle or antenna

visibility are often suboptimal for deep locations and/or large patients. Lesions are obscured by gas bubble or ice-ball formation during thermal ablation. Electromagnetic tracking of ablation devices and fusion between real-time ultrasound and pre-procedural CT, MRI or PET/CT have shown to facilitate targeting of lesions that are sonographically invisible [5]. This solution requires dedicated software, hardware and disposables, and does not solve the limitations related to ultrasound for direct thermal ablation monitoring. CT guidance offers intra-procedural volumetric imaging with usually superior lesion and peritumoral environment visibility [6]. Contrast-enhanced CT can be used for planning and for monitoring of the ablation zone. Due to limited possibility of gantry tilting, the use of CT to target lesions that require multiple-angulated trajectories may be challenging. In addition, real time requires CT fluoroscopy which is not always available and leads to a significant increase in radiation exposure to the patient and operator. PET/CT and MRI guidance are emerging options for percutaneous tumor ablation, offering real-time imaging, excellent tumor visibility and novel approaches in ablation monitoring [7, 8]. However, limited accessibility and increased associated costs have currently limited the use of these modalities to dedicated centers and research institutions.

C-arm cone-beam computed tomography (CBCT) is a new imaging technology that enables acquisition of cross-sectional imaging with modern angiographic systems equipped with a flat panel detector [9]. Volumetric tomographic images can be combined and co-displayed with conventional 2D angiographic imaging and dedicated software during interventional procedures to plan treatment, navigate/position the catheter or device, monitor the treatment, and assess the final result or verify margins. In this paper, we highlight the technical aspects and clinical applications of CBCT imaging and navigation and explore its utility for common loco-regional oncological treatments.

Technique

Acquisition and injection protocols

CBCT imaging is based on a rotational projection acquisition using the motorized C-shaped gantry (Fig. 1) [10]. To enable tomographic reconstruction, X-ray projection images of the object are acquired along a circular path covering at least 180° rotation. The target area is positioned in the center of rotation (isocenter). Volumetric CBCT images are obtained using 3D cone-beam image reconstruction [11]. The motion path includes an acceleration and deceleration phase encompassing a phase of constant speed of 30–60° per second (s) and projection acquisition is performed in pulsed mode. A complexity for tomographic reconstruction on interventional C-arm systems is the need to accurately measure the true system position, which needs to be taken into account during back-projection. This is determined from the geometric calibration [12]. For abdominal imaging, typical tube parameters are 5–10 ms pulses per projection at 120 kV tube voltage including copper filtration with frame rates of 30–60° frames per sec. Recent detectors cover a planar region of 30 × 40 cm at a high spatial resolution up to 150^2 μm^2 [12]. Projection acquisition includes the use of one-dimensional anti-scatter grids to suppress scattered photons. To generate images with CT like quality, Parker weighting and correction methods (e.g. projection truncation, scatter, and beam hardening) need to be included. Cone-beam filtered

back-projection is applied as image reconstruction [10]. Patient dose considerations result in practical CBCT spatial resolution of the order of $0.5 \times 0.5 \times 0.5$ mm^3, which are achieved by adapting the focal spot size, detector readout resolution, and the reconstruction filter. The decrease in the rotation time of the C-arm systems in recent years from almost 20 s down to 3–4 s enables multi-phasic acquisitions of contrast studies, as they are used in liver or brain studies today [13, 14] (Fig. 2).

Patient preparation and equipment setup

The patient should be positioned on the angiographic table so that the anatomy of interest can be included in the CBCT field of view (FOV = $25 \times 25 \times 19$ cm) and that the C-arm can rotate around the patient with the flat panel detector in landscape mode. Off-center patient positioning should be considered especially for patients with lesions at the periphery, obese patients or with marked hepatomegaly. Satisfactory offset (off-midline, to include skin entry) should be taken into account for percutaneous procedures.

Ceiling-mounted monitors and radiation shields should be arranged so that they can be promptly moved and CBCT imaging can be performed safely. Contrast injector and other devices such as ECG box, infusion poles, blood pressure cuffs, etc. should be positioned caudally from the C-arm to keep clear from the rotation trajectory. Long cables with low radio-opacity should be used to allow unobstructed longitudinal table movements. Any object in the CBCT FOV, including jewelry, ECG leads or other radiopaque sensors, should be removed or repositioned. Armrest accessories are recommended if available to improve patient comfort during CBCT imaging, but should not obstruct rotational movements [15].

Radiation exposure

The X-ray exposure associated to CBCT has been the subject of several studies performed on phantoms, animals, patients and the medical team [16-19]. The X-ray exposure may vary between manufacturers depending on parameters such as kVs, mAs, filter thickness and material, and number of projections. The estimated effective dose to the patient for one CBCT scan of the abdomen is approximately 3–10 mSv, generally lower than the comparable dose in an abdominal MDCT scan (10–12 mSv) [16, 20]. As for all interventional procedures using X-ray exposure, the operators should wear protective devices and leave the examination room when performing 3D scans, and CBCT acquisition should be used judiciously.

Therapy planning and navigation software

The availability of volumetric datasets showing tumor location, vascular territory and parenchymal environment at the time of the procedure provides an excellent platform to define a safe and effective route to the lesion and guide device positioning. The volumetric data are also amenable to multimodality or multi-phase fusion. Therapy planning software for both intra-arterial (chemo/radio) embolization and percutaneous ablation is commercially available and fully integrated with C-arm systems. Intra-arterial therapy planning software (EmboGuide, Philips Healthcare or Flight Plan for Liver, GE Healthcare) is capable to automatically identify the feeding arteries to the targeted lesion(s). The basic workflow involves the 3D segmentation of the targeted lesion(s) on the CBCT dataset and the

automatic extraction of candidate feeders from a starting point (normally the micro-catheter tip) to the targets. The use of a delayed parenchymal CBCT is often recommended for optimal tumor boundary delineation [21]. Needle planning software (XperGuide Ablation, Philips Healthcare or Innova TrackVision, GE Healthcare or iGuide, Siemens Healthcare) provides a simple technique to define the needle trajectory from the skin entry point to the target. The needle paths can be drawn in any direction and multiple paths can be concurrently shown [22].

CBCT datasets are acquired in a calibrated space where the position of the acquired 3D dataset is known with respect to the X-ray beam generation and the mechanical movements of both C-arm and angiographic table. This allows super-imposing the live fluoroscopy stream on a 3D rendering of the CBCT dataset including the graphics from the therapy plan. The 3D dataset and the needle or feeding vessel paths follow the rotation and angulation movements of the C-arm, translations of the table, and automatically adjusts to magnification changes. The operator can then follow the graphical overlays for device manipulation and/or automatically move the C-arm into pre-defined positions that facilitate catheterization or accurate needle alignment towards the targeted lesion(s).

Clinical applications

CBCT and embolotherapy

Transarterial chemoembolization—The use of CBCT in the visualization and localization of hepatic lesions at the time of intervention is crucial for effective intra-arterial therapy in seeing and reaching the lesion and in assessing response [21]. DSA can provide excellent vascular visualization but it has less sensitivity for tumor detection than CT or CBCT due to its low soft-tissue contrast and 2D projection nature [15, 23-28]. This can also limit the identification of feeding vessels to tumor [29-31]. CBCT with its 3D nature, soft-tissue contrast, and especially coupled with post-processing software is superior to DSA in lesion detection and tumor feeding vessel identification [23, 30-37]. Figure 3 shows multimodality matching of a target HCC lesion in the pre-TACE MR with post-DEB delivery CBCT, confirming delivery of the DEB-contrast medium mixture. The intra-procedural DSA shows only a blush of the lesion. The role of CBCT can also be seen in therapy response assessment, in particular for Lipiodol deposition (Fig. 4) [27, 38-41] or for marginal contrast retention with DEB, which is associated with successful treatment outcomes 1 month post-DEB [27].

A more recent development is the Dual Phase CBCT, where a bi-phasic CBCT is acquired using a single contrast injection. Dual phase has increased tumor detection versus single-phase CBCT alone and is comparable to the gold standard of contrast-enhanced MDCT and MRI in lesion detection and in predicting therapy response [28, 42, 43]. With these highlights of CBCT in lesion detection, tumor feeding vessel identification, and therapy assessment, the addition of CBCT along with DSA can prolong patient survival [44].

Selective internal radiation therapy—Selective internal radiation therapy (SIRT) is a relatively new, catheter-directed treatment modality of both primary [45] and secondary [46, 47] liver tumors. In contrast to transarterial chemoembolization (TACE), an angiographic

work-up is required prior to yttrium-90 (Y-90) loaded microsphere infusion into the hepatic artery [48]. Angiographic work-up mainly consists in identifying (and, if indicated, coil-embolizing) hepatoenteric arteries, originating from the hepatic arteries [49]; defining the vascular territory of all targeted hepatic arteries; and identifying the tumoral lesions within these vascular territories. Additionally, total volume calculation of the hepatic vascular territory and targeted liver tumors is important to correctly calculate the total dose of yttrium-90 microspheres to be injected in the targeted hepatic arteries (Fig. 5), as well as fraction shunted to lung.

Digital subtraction angiography (DSA) is the gold standard to identify hepatoenteric arteries. However, Louie et al. [50] demonstrated that CBCT identified extrahepatic contrast enhancement in 52 % of cases. In 33 % of cases these additional CBCT observations, not demonstrated by DSA, lead to additional coil embolization and/or change in catheter position. Finally, in 19 % of cases, extrahepatic enhancement was, even in retrospect, not detected by Tc99-MAA imaging.

Total liver, lobar, and tumor volume measurements are typically performed based on conventional CT or MRI. However, parts of tumoral mass lesions located in the right or left liver lobe might be vascularized by the contralateral hepatic artery, which, potentially, might lead to miscalculation of the liver and tumor volume and finally might result in over- or undertreatment of one or both liver lobes resulting in suboptimal clinical outcome (Fig. 6). CBCT depicts perfused tissue location, which is essential for correct segment classification or pre-treatment portal vein embolization.

Renal embolization—Arterial embolization indications in oncologic kidney therapy are uncommon with the success of partial nephrectomy and percutaneous ablation. The main indications are embolization of hypervascular cancers and associated renal vein thrombosis to limit blood loss during renal cell carcinoma (RCC) surgery [51], or to primarily treat or prevent hemorrhage risk for angiomyolipoma (AML) [52].

AML is a common benign renal tumor. The major risk of AML is retroperitoneal hemorrhage by spontaneous rupture of intratumoral aneurysms. Treatment is recommended when tumor size exceeds 4 cm, when aneurysms, symptoms, or hemorrhage history is present [53, 54]. The first line of treatment is angiographic embolization that needs to be selective and nephron-sparing. Identification of feeder vessels is required and can be optimized using CBCT with catheter injection from the renal artery and dedicated automatic vessel detection software. Automatic vessel detection software has shown efficiency during TACE [30-32] and can also facilitate AML embolization since specific tissue geographies supplied by specific vessels can be exquisitely mapped out (Figs. 7, 8, 9).

Prostate embolization—Prostate arterial embolization (PAE) is an emerging arterial embolization technique for the treatment of benign prostate hyperplasia [55-57] and could become an experimental alternative option to surgery, especially for patients who refuse surgery. Left and right prostatic arteries (PA) are em-bolized when possible during the same procedure. CBCT has shown potential utility in this procedure to avoid untargeted vessel

embolization (inferior vesical artery or rectal artery with subsequent collateral off-target damage) and to optimize catheter placement and selective embolization [58].

The role of dual-phase CBCT with automatic vessel detection software (EmboGuide, Philips Healthcare) during PAE may define vessels and perfused tissue territory. Dual-Phase CBCT can be acquired using the following protocol: 24 cc of iodine contrast at 2 cc/s, delay 4 s, considering a single CBCT scan duration of 8 s. The arterial phase CBCT is acquired with a 4 s delay after contrast injection, while the delayed phase CBCT is obtained 5 s after the end of the first CBCT scan. Figure 10 shows well-visible prostatic enhancement, especially on the delayed phase, enabling 3D prostate segmentation for software-assisted detection of its arterial supply (Fig. 11). Software-assisted detection of prostatic vessels is feasible and collateral non-target vessels may also be successfully depicted on CBCT.

CBCT and tumor ablation

Image-guided percutaneous ablation is a minimally invasive, therapeutic option for localized disease. Recurrence and survival rates depend on complete ablation of the entire tumor including a sufficient margin of surrounding healthy tissue [59].

CBCT may provide a guidance method for ablation procedures and enables ablation procedures requiring CT guidance to be performed in the interventional fluoroscopy/ angiography suite, without requiring a CT and without impacting workflow, especially in facilities without a dedicated IR CT [60].

As with embolotherapy, CBCT can assist in all steps of thermal ablation (planning, positioning needles, ablation monitoring, modification of needle plan, post-ablation assessment and verification of completion) for both thoracic and abdominal tumors. For thoracic tumors, respiratory gating may minimize motion mis-registration, thus facilitating navigation.

Indeed, once the patient is positioned on the angio-graphic table, a pre-procedural CBCT is performed to visualize the target lesion and plan the procedure.

The operator can segment the lesion and determine the skin entry point as well as the target. Information for procedure planning including ablation device path, depth and required number of probes can be obtained (Fig. 12). Some software versions also allow overlay of the manufacturer-specified ablation area superimposed on the segmented lesion, to assist in determining the number and location of subsequent ablation probes needed to obtain a safe ablation zone and a complete coverage of lesion. (Fig. 13) The ablation isotherms can interact with 3D lesion segmentation, multimodality-defined tumor, and user-defined safety margins (when available) to identify potential areas of undertreatment (or “tumor at risk for undertreatment”).

Once the planning is completed, the probes are advanced under guidance of the co-registered CBCT and fluoroscopy. A CBCT is repeated to confirm correct probe positioning, (Fig. 14) or to adjust the plan based upon actual needle location.

Once the ablation is complete, repeat CBCT is performed to rule out peri-procedural complications such as a pneumothorax following a lung ablation (Fig. 15) and to assess the adequacy of the ablation zone. Previous literature concerning CBCT-guided lung and bone biopsies demonstrated that unenhanced pre-procedural CBCT is sufficient to delineate the lesion and enable segmentation [22, 61]. The same could be applied in ablation cases [62]; for difficult lung ablations close to vital structures, a contrast enhancement CBCT may be needed.

Most abdominal ablations will also require a contrast-enhanced CBCT pre-procedurally and post-procedurally. Several techniques are possible for contrast injection during CBCT scan.

In a preliminary study, Morimoto et al. [63] suggested the use of intra-arterial contrast-enhanced CBCT to optimize liver lesion conspicuity for ablation and to monitor therapy. All five patients were successfully treated at 1 month; however, this requires catheterization of the hepatic artery. Peripheral intravenous injection is an alternative option which is the method used by the authors during the pre-procedural CBCT (data unpublished) to provide an optimal visualization of lesion target (both hepatic and renal tumors) and adjacent structures, used for ablation planning.

Moreover, in a preliminary series including 12 hepatic lesions treated with RFA, Iwzawa et al. [64] concluded the efficacy of intravenous contrast-enhanced C-arm CT for assessing ablative areas and safety margins immediately after treatment is nearly equivalent to that of MDCT performed 3–7 day after RFA.

Contrast-enhanced CBCT can be avoided in cases of contrast allergy or renal failure. Fusion of MRI or PET to the CBCT may be helpful to define tumor or vessels in these cases. As described by Abi-Jaoudeh et al. [65], previous diagnostic imaging such as contrast-enhanced CT, PET-CT or MRI can be co-registered with unen-hanced pre-procedural CBCT to plan the procedure and with the post-procedural CBCT to assess the completion of the ablation.

C-arm CBCT intrinsically has also potential disadvantages in terms of contrast resolution, image quality and FOV. However, the use of co-registration/fusion with diagnostic imaging or enhanced or other phase-enhanced CBCT may overcome some of these limitations [66].

In addition, the image quality can also be affected by motion artifacts; thus, patient setup and support staff training are vital to improve image quality [67].

Conclusion

CBCT imaging is a new and empowering imaging technology to add to the arsenal of the interventional radi-ologist/interventional oncologist. Given the current body of evidence for transarterial chemoembolization and promising future applications such as radioembolization and prostatic arterial embolization, CBCT is expected to become a mainstay imaging modality in tumor embolo-therapy. Initial results on percutaneous tumor ablation are promising but more evidence is required to establish its role for different clinical applications. Multimodality navigation, semi-automatic fusion, semi-automatic vessel detection, dual-phase CBCT, ablation planning, and synergy with ultrasound are early

and emerging options, whose added values and potential advantages are in the process of being defined.

Certainly, CBCT is one of the most interesting and empowering IR/IO tools to emerge in recent times.

Acknowledgments

This study supported in part by the Intramural Research Program of the NIH and the NIH Center for Interventional Oncology (BJW & NAJ). NIH and Philips Healthcare have a cooperative research and development agreement.

References

1. Solomon SB, Silverman SG. Imaging in interventional oncology. Radiology. 2010; 257(3):624–640. [PubMed: 21084414]
2. Abi-Jaoudeh N, Duffy AG, Greten TF, Kohn EC, Clark TW, Wood BJ. Personalized oncology in interventional radiology. J Vasc Interv Radiol. 2013; 24(8):1083–1092. [PubMed: 23885909]
3. Chen X, Xiao E, Shu D, Yang C, Liang B, He Z, Bian D. Evaluating the therapeutic effect of hepatocellular carcinoma treated with transcatheter arterial chemoembolization by magnetic resonance perfusion imaging. Eur J Gastroenterol Hepatol. 2014; 26(1):109–113. [PubMed: 24284371]
4. Kim I, Kim DJ, Kim KA, Yoon SW, Lee JT. Feasibility of MDCT angiography for determination of tumor-feeding vessels in chemoembolization of hepatocellular carcinoma. J Comput Assist Tomogr. 2014 [Epub ahead of print].
5. Buckner CA, Venkatesan A, Locklin JK, Wood BJ. Realtime sonography with electromagnetic tracking navigation for biopsy of a hepatic neoplasm seen only on arterial phase computed tomography. J Ultrasound Med. 2011; 30(2):253–256. [PubMed: 21266564]
6. Park BJ, Byun JH, Jin YH, Won HJ, Shin YM, Kim KW, Park SJ, Kim PN. CT-guided radiofrequency ablation for hepato-cellular carcinomas that were undetectable at US: therapeutic effectiveness and safety. J Vasc Interv Radiol. 2009; 20(4):490–499. [PubMed: 19328427]
7. Ryan R, Sofocleous C, Schöder H, et al. Split-dose technique for FDG PET/CT-guided percutaneous ablation: a method to facilitate lesion targeting and to provide immediate assessment of treatment effectiveness. Radiology. 2013 doi:10.1148/radiol.13121462.
8. Tuncali K, Morrison PR, Winalski CS, Carrino JA, Shankar S, Ready JE, vanSonnenberg E, Silverman SG. MRI-guided percutaneous cryotherapy for soft-tissue and bone metastases: initial experience. Am J Roentgenol. 2007; 189(1):232–239. [PubMed: 17579176]
9. Orth RC, Wallace MJ, Kuo MD, et al. Technology assessment committee of the society of interventional Radiology C-arm cone-beam CT: general principles and technical considerations for use in interventional radiology. J Vasc Interv Radiol. 2008; 19(6):814–820. [PubMed: 18503894]
10. Grass, M.; Guillemaud, R.; Rasche, V. Interventional X-ray volume tomography. In: Grangeat, P., editor. Tomography. Wiley; New York: 2009. p. 287-306.
11. Racadio JM, Babic D, Homan R, et al. Live 3D guidance in the interventional radiology suite. Am J Roentgenol. 2007; 189(6):W357–W364. [PubMed: 18029850]
12. Grass M, Koppe R, Klotz E, et al. Three-dimensional reconstruction of high contrast objects using C-arm image inten-sifier projection data. Comput Med Imaging Graph. 1999; 23(6):311–321. [PubMed: 10634143]
13. Lin M, Loffroy R, Noordhoek N, et al. Evaluating tumors in transcatheter arterial chemoembolization (TACE) using dual-phase cone-beam CT. Minim Invasive Ther Allied Technol. 2011; 20(5):276–281. [PubMed: 21082901]
14. Caroff J, Jittapiromsak P, Ruijters D, et al. Use of time attenuation curves to determine steady-state characteristics before C-arm CT measurement of cerebral blood volume. Neuroradiology. 2014; 56(3):245–249. [PubMed: 24449134]

15. Tognolini A, Louie J, Hwang G, et al. C-arm computed tomography for hepatic interventions: a practical guide. J Vasc Interv Radiol. 2010; 21(12):1817–1823. [PubMed: 20970354]
16. Kothary N, Abdelmaksoud MH, Tognolini A, et al. Imaging guidance with C-arm CT: prospective evaluation of its impact on patient radiation exposure during transhepatic arterial chemoembolization. J Vasc Interv Radiol. 2011; 22(11):1535–1543. [PubMed: 21875814]
17. Schulz B, Heidenreich R, Heidenreich M, et al. Radiation exposure to operating staff during rotational flat-panel angiog-raphy and C-arm cone beam computed tomography (CT) applications. Eur J Radiol. 2012; 81(12):4138–4142. [PubMed: 22304981]
18. Suzuki S, Yamaguchi I, Kidouchi T, Yamamoto A, Masumoto T, Ozaki Y. Evaluation of effective dose during abdominal three-dimensional imaging for three flat-panel-detector angiog-raphy systems. Cardiovasc Intervent Radiol. 2011; 34(2):376–382. [PubMed: 20495804]
19. Paul J, Jacobi V, Farhang M, Bazrafshan B, et al. Radiation dose and image quality of X-ray volume imaging systems: cone-beam computed tomography, digital subtraction angiography and digital fluoroscopy. Eur Radiol. 2013; 23(6):1582–1593. [PubMed: 23250112]
20. Braak SJ, van Strijen MJ, van Es HW, Nievelstein RA, van Heesewijk JP. Effective dose during needle interventions: cone-beam CT guidance compared with conventional CT guidance. J Vasc Interv Radiol. 2011; 22(4):455–461. [PubMed: 21463755]
21. Tacher V, Radaelli A, Lin M, et al. How i do it: cone beam computed tomography during transarterial chemoembolization for liver cancer. Radiology. 2014 Accepted.
22. Floridi C, Muollo A, Fontana F, et al. C-arm cone-beam computed tomography needle path overlay for percutaneous biopsy of pulmonary nodules. Radiol med. 2014 [Epub ahead of print].
23. Wallace MJ, Murthy R, Kamat PP, et al. Impact of C-arm CT on hepatic arterial interventions for hepatic malignancies. J Vasc Interv Radiol. 2007; 18(12):1500–1507. [PubMed: 18057284]
24. Wallace MJ, Kuo MDK, Glaiberman C, et al. Three-dimensional C-arm cone-beam CT:applications in the interventional suite. J Vasc Interv Radiol. 2008; 19:799–813. [PubMed: 18503893]
25. Wallace MJ. C-arm computed tomography for guiding hepatic vascular interventions. Tech Vasc Interv Radiol. 2007; 10(1):79–86. [PubMed: 17980322]
26. Hirota S, Nakao N, Yamamoto S, et al. Cone-beam CT with flat-panel-detector digital angiography system: early experience in abdominal interventional procedures. Cardiovasc Intervent Radiol. 2006; 29(6):1034–1038. [PubMed: 16988877]
27. Suk, OhJ; Jong Chun, H., et al. Transarterial chemoemboli-zation with drug-eluting beads in hepatocellular carcinoma: usefulness of contrast saturation features on cone-beam computed tomography imaging for predicting short-term tumor response. J Vasc Interv Radiol. 2013; 24(4): 483–489. [PubMed: 23452553]
28. Miyayama S, Yamashiro M, Okuda M, et al. Detection of corona enhancement of hypervascular hepatocellular carcinoma by C-arm dual-phase cone-beam CT during hepatic arteriography. Cardiovasc Intervent Radiol. 2011; 34(1):81–86. [PubMed: 20333382]
29. Meyer B, Witschel M, Frericks B, et al. The value of combined soft-tissue and vessel visualisation before transarterial chemoembolisation of the liver using C-arm computed tomography. Eur Radiol. 2009; 19(9):2302–2309. [PubMed: 19424701]
30. Deschamps F, Solomon S, Thornton R, et al. Computed analysis of three-dimensional cone-beam computed tomography angiography for determination of tumor-feeding vessels during chemoembolization of liver tumor: a pilot study. Cardiovasc Intervent Radiol. 2010 [Epub ahead of print].
31. Miyayama S, Yamashiro M, Okuda, et al. Usefulness of cone-beam computed tomography during ultraselective trans-catheter arterial chemoembolization for small hepatocellular carcinomas that cannot be demonstrated on angiography. CardioVasc Intervent Radiol. 2009; 32(2):255–264. [PubMed: 19067043]
32. Iwazawa J, Ohue S, Hashimoto N, et al. Clinical utility and limitations of tumor-feeder detection software for liver cancer embolization. Eur J Radiol. 2013; 82(10):1665–1671. [PubMed: 23743053]

33. Tacher V, Lin M, Bhagat N, et al. Dual-phase cone-beam computed tomography to see, reach, and treat hepatocellular carcinoma during drug-eluting beads transarterial chemoembolization. J Vis Exp. 2013; 2(82):50795. [PubMed: 24326874]
34. Higashihara H, Osuga K, Onishi H, et al. Diagnostic accuracy of C-arm CT during selective transcatheter angiography for hepa-tocellular carcinoma: comparison with intravenous contrast-enhanced, biphasic, dynamic MDCT. Eur Radiol. 2012
35. Yu MH, Kim JH, Yoon J-H, et al. Role of C-arm CT for transcatheter arterial chemoembolization of hepatocellular carcinoma: diagnostic performance and predictive value for therapeutic response compared with gadoxetic acid-enhanced MRI. Am J Roentgenol. 2013; 201(3):675–683. [PubMed: 23971463]
36. Miyayama S, Matsui O, Yamashiro M, et al. Detection of hepatocellular carcinoma by CT during arterial portography using a cone-beam CT technology: comparison with conventional CTAP. Abdom Imaging. 2009; 34:502–506. [PubMed: 18373115]
37. Iwazawa J, Ohue S, Hashimoto N, et al. Detection of hepatocellular carcinoma: comparison of angiographic C-arm CT and MDCT. Am J Roentgenol. 2010; 195(4):882–887. [PubMed: 20858813]
38. Wang Z, Lin M, Lesage D, et al. Three-dimensional evaluation of lipiodol retention in HCC after chemoembolization: a quantitative comparison between CBCT and MDCT. Acad Radiol. 2014; 21(3):393–399. [PubMed: 24507426]
39. Chen R, Geschwind J-F, Wang Z, et al. Quantitative assessment of lipiodol deposition after chemoembolization: comparison between cone-beam CT and multi-detector CT. J Vasc Interv Radiol. 2013; 24(12):1837–1844. [PubMed: 24094672]
40. Jeon UB, Lee JW, Choo KS, et al. Iodized oil uptake assessment with cone-beam CT in chemoembolization of small hepatocellular carcinomas. World J Gastroenterol. 2009; 15(46): 5833–5837. [PubMed: 19998505]
41. Iwazawa J, Ohue S, Kitayama T, et al. C-arm CT for assessing initial failure of iodized oil accumulation in chemoembolization of hepatocellular carcinoma. Am J Roentgenol. 2011; 197(2):W337–W342. [PubMed: 21785062]
42. Loffroy R, Lin M, Yenokyan G, et al. Intraprocedural C-arm dual-phase cone-beam CT: can it be used to predict short-term response to TACE with drug-eluting beads in patients with hepatocellular carcinoma? Radiology. 2013; 266(2):636–648. [PubMed: 23143027]
43. Loffroy R, Lin M, Rao P, et al. Comparing the detectability of hepatocellular carcinoma by C-arm dual-phase cone-beam computed tomography during hepatic arteriography with conventional contrast-enhanced magnetic resonance imaging. Cardiovasc Intervent Radiol. 2012; 35(1):97–104. [PubMed: 21328023]
44. Iwazawa J, Ohue S, Hashimoto N, et al. Survival after C-arm CT-assisted chemoembolization of unresectable hepatocellular carcinoma. Eur J Radiol. 2012; 81(12):3985–3992. [PubMed: 22959287]
45. Sato K, Lewandowski R, Mulcahy M, et al. Unrespectable chemo refractory liver metastases: radioembolization with 90Y microspheres: safety, efficacy and survival. Radiology. 2008; 247:507–515. [PubMed: 18349311]
46. Salem R, Lewandowski R, Mulcahy M, et al. Radioemb-olization for hepatocellular carcinoma using Yttrium-90 micro-spheres: a comprehensive report of long-term outcomes. Gastroenterology. 2010; 138:52–64. [PubMed: 19766639]
47. Hendlisz A, Van den Eynde M, Peeters M, et al. Phase III trial comparing protracted intravenous fluorouracil infusion alone or with yttrium-90 resin microspheres radioembolization for liver-limited metastatic colorectal cancer refractory to standard chemotherapy. J Clin Oncol. 2010; 28:3687–3694. [PubMed: 20567019]
48. Maleux G, Heye S, Vaninbroukx J, et al. Angiographic considerations in patients undergoing liver-directed radioembo-lization with 90Y microspheres. Acta Gastroenterol Belg. 2010; 73:489–496. [PubMed: 21299160]
49. Heusner T, Hamami M, Ertle J, et al. Angiography-based C-arm CT for the assessment of extrahepatic shunting before radioembolization. Rofo. 2010; 182:603–608. [PubMed: 20183775]

50. Louie J, Kothary N, Kuo W, et al. Incorporating cone-beam CT into the treatment planning for Yttrium-90 radioembolization. J Vasc Intervent Radiol. 2009; 20:606–613.
51. Bakal CW, Cynamon J, Lakritz PS, Sprayregen S. Value of preoperative renal artery embolization in reducing blood transfusion requirements during nephrectomy for renal cell carcinoma. J Vasc Interv Radiol. 1993; 4(6):727–731. [PubMed: 8280991]
52. Ramon J, Rimon U, Garniek A, et al. Renal angiomyoli-poma: long-term results following selective arterial embolization. Eur Urol. 2009; 55(5):1155–1161. [PubMed: 18440125]
53. Chan CK, Yu S, Yip S, Lee P. The efficacy, safety and durability of selective renal arterial embolization in treating symptomatic and asymptomatic renal angiomyolipoma. Urology. 2011; 77(3):642–648. [PubMed: 21131030]
54. Chatziioannou A, Gargas D, Malagari K, et al. Transcath-eter arterial embolization as therapy of renal angiomyolipomas: the evolution in 15 years of experience. Eur J Radiol. 2012; 81(9):2308–2312. [PubMed: 21708442]
55. Gao YA, Huang Y, Zhang R, et al. Benign prostatic hyperplasia: prostatic arterial embolization versus transurethral resection of the prostate—a prospective, randomized, and controlled clinical trial. Radiology. 2014; 270(3):920–928. [PubMed: 24475799]
56. Pisco J, Campos Pinheiro L, Bilhim T, et al. Prostatic arterial embolization for benign prostatic hyperplasia: short- and intermediate-term results. Radiology. 2013; 266(2):668–677. [PubMed: 23204546]
57. Bilhim T, Pisco J, Rio Tinto H, et al. Unilateral versus bilateral prostatic arterial embolization for lower urinary tract symptoms in patients with prostate enlargement. Cardiovasc Intervent Radiol. 2013; 36(2):403–411. [PubMed: 23232858]
58. Bagla S, Rholl KS, Sterling KM, et al. Utility of cone-beam CT imaging in prostatic artery embolization. J Vasc Interv Radiol. 2013; 24(11):1603–1607. [PubMed: 23978461]
59. Widmann G, Bodner G, Bale R, et al. Tumour ablation: technical aspects. Cancer Imaging. 2009; 9:S63–S67. [PubMed: 19965296]
60. Carrafiello G, Mangini M, De Bernardi I, et al. Microwave ablation therapy for treating primary and secondary lung tumours: technical note. Radiol Med. 2010; 115:962–974. [PubMed: 20352357]
61. Carrafiello G, Fontana F, Mangini M, et al. Initial experience with percutaneous biopsies of bone lesions using XperGuide cone-beam CT (CBCT): technical note. Radiol Med. 2012; 117(8):1386–1397. [PubMed: 22327915]
62. Busser WM, Braak SJ, Fiitterer JJ, et al. Cone beam CT guidance provides superior accuracy for complex needle paths compared with CT guidance. Br J Radiol. 2013; 86(1030):310–318.
63. Morimoto M, Numata K, Kondo M, et al. C-arm cone beam CT for hepatic tumor ablation under real-time 3D imaging. Am J Roentgenol. 2010; 194(5):W452–W454. [PubMed: 20410393]
64. Iwazawa J, Ohue S, Hashimoto N, et al. Ablation margin assessment of liver tumors with intravenous contrast-enhanced C-arm computed tomography. World J Radiol. 2012; 4(3):109–114. [PubMed: 22468192]
65. Abi-Jaoudeh N, Mielekamp P, Noordhoek N, et al. Cone-beam computed tomography fusion and navigation for real-time positron emission tomography-guided biopsies and ablations: a feasibility study. J Vasc Interv Radiol. 2012; 23(6):737–743. [PubMed: 22494658]
66. Abi-Jaoudeh N, Kruecker J, Kadoury S, et al. Multimodality image fusion-guided procedures: technique, accuracy, and applications. Cardiovasc Intervent Radiol. 2012; 35(5):986–998. [PubMed: 22851166]
67. Abi-Jaoudeh N, Kobeiter H, Xu S, Wood BJ. Image fusion during vascular and nonvascular image-guided procedures. Tech Vasc Interv Radiol. 2013; 16(3):168–176. [PubMed: 23993079]

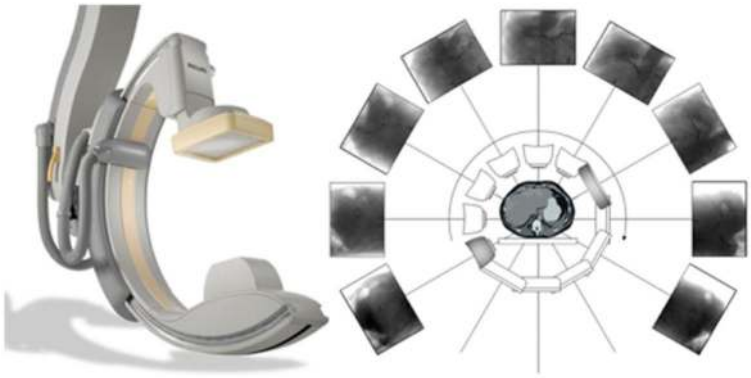

Fig. 1.
CBCT imaging is based on the rotation of a C-arm equipped with a flat panel detector (*left image*) around the patient. 2D projections are acquired (*right image*) and reconstructed to generate a 3D volumetric data set

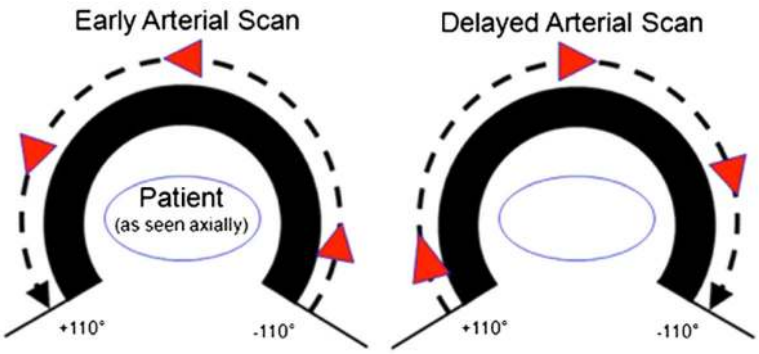

Fig. 2.

Schematic representation of a dual-phase CBCT acquisition as it is used for TACE procedures

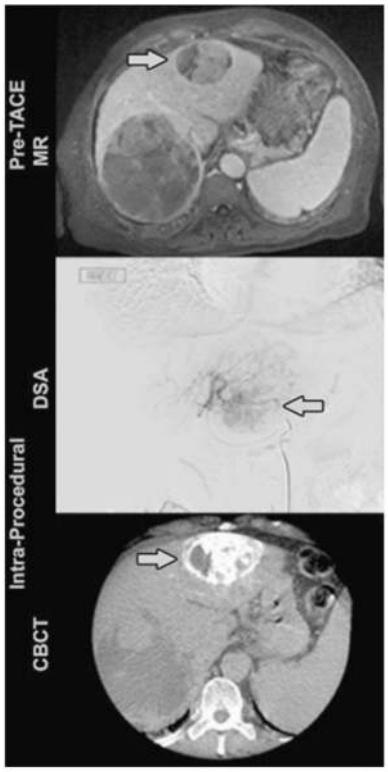

Fig. 3.

74-year-old male with HCC based on imaging findings and elevated AFP level. NASH and cirrhosis etiology. Child-Pugh class B, BCLC B, ECOG 0. The *arrow* indicates the target lesion that was treated with DEBs. Note the matching of the lesion in the pre-TACE MR with the intra-procedural CBCT post-DEB delivery

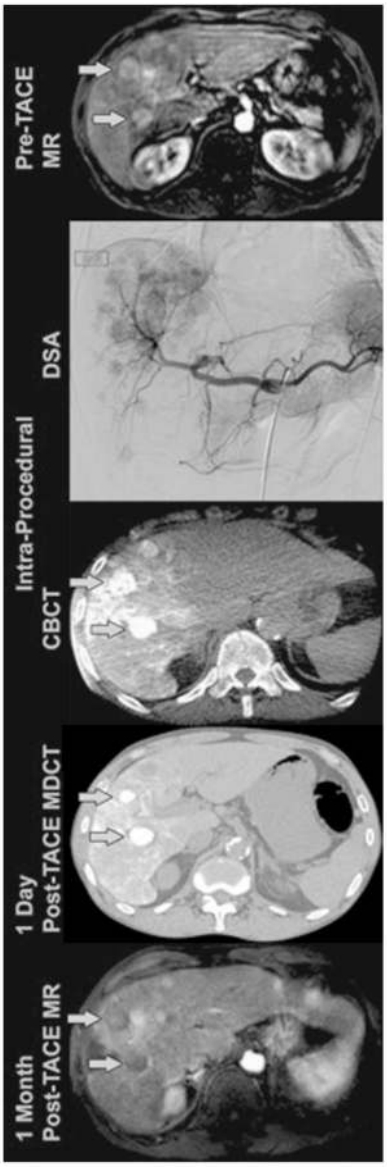

Fig. 4.

55-year-old male patient with biopsy proven HCC. Hepatitis C and cirrhosis etiology. Child-Pugh class A, BCLC B, ECOG 0. The *arrows* indicate the lesions targeted with delivery of Lipiodol. Note that the lesion depiction on the pre- and intra-procedural imaging matches with the post-TACE imaging, and especially with the hypoenhancement 1 month post-TA

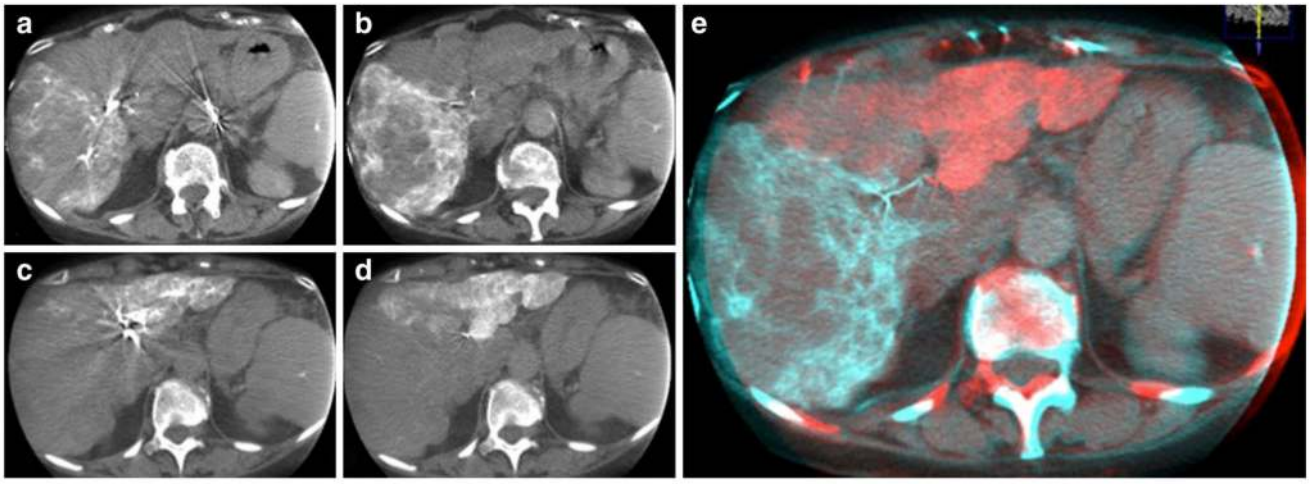

Fig. 5.

a–e Diffuse metastatic tumoral involvement of both liver lobes in a 67-year-old woman presenting with chemorefractory liver metastases from breast carcinoma. Angiographic work-up prior to Y90-radioembolization included CBCT imaging demonstrating the vascular territory of right and left liver lobe. The vascular territory of both hepatic arteries does not fully agree with the morphological division into the right and left liver lobe

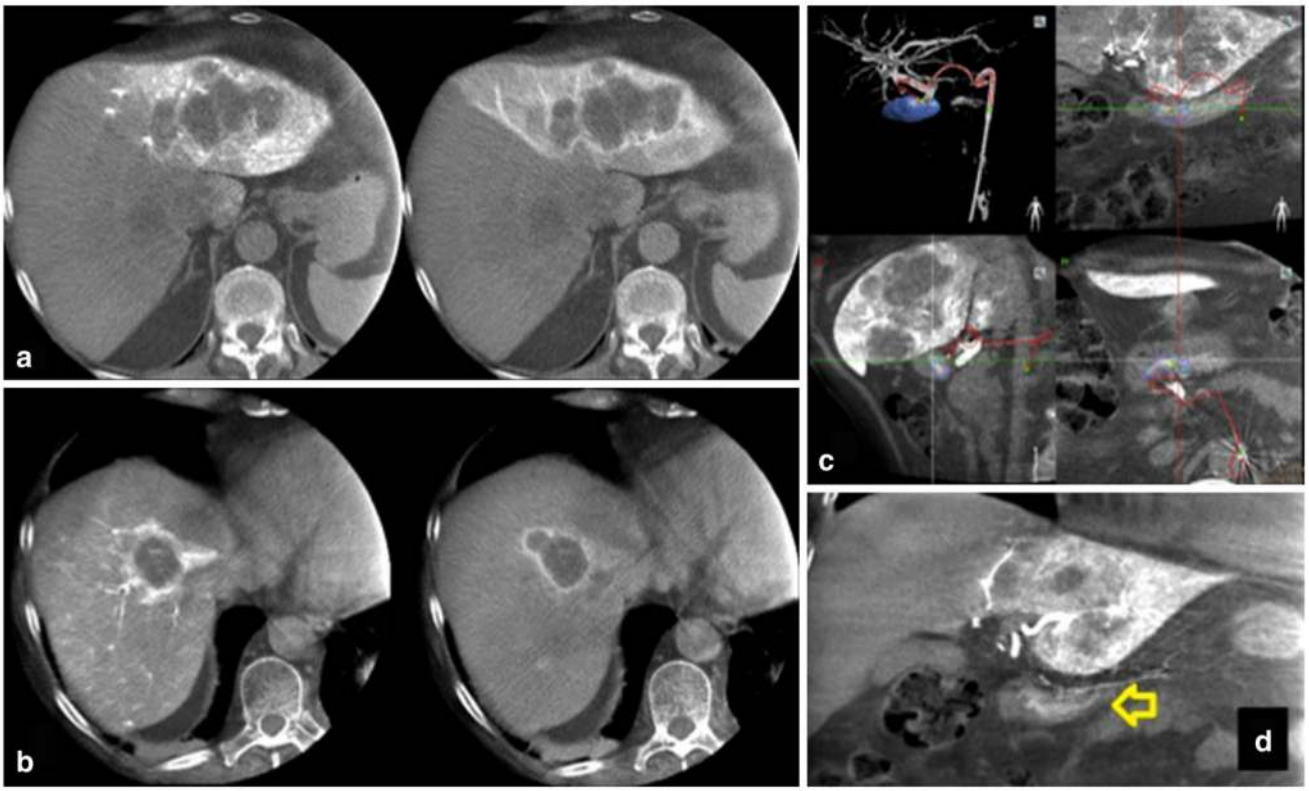

Fig. 6.

a–d CBCT imaging during Y90 work-up in a 60-year-old patient suffering from chemorefractory colorectal liver metastases clearly shows a small hepatoenteric vessel, feeding the gastric wall: right gastric artery. Using Emboguide, the small hepatoenteric vessel was identified on angiography. Subsequently, proximal coil emboli-zation of the right gastric artery was performed

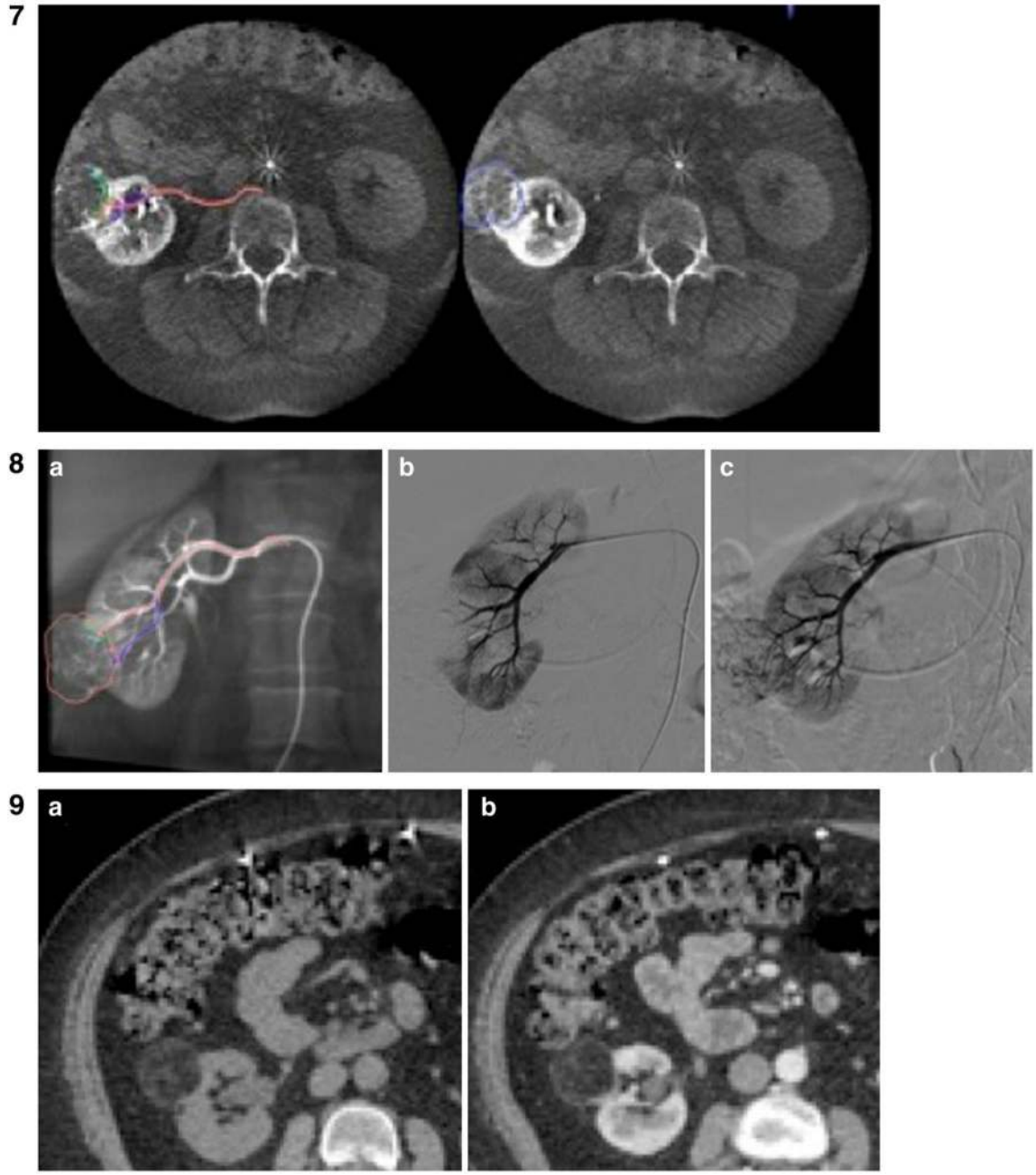

Figs. 7-9.

Angiomyolipoma embolization. AML was segmented on enhanced CBCT (7). Emboguide software automatically detected feeder vessels (**8a**). Embolization was performed in those vessels (**8b**). At the end of the procedure, 2D angiography showed devascularization of the lesion (**8c**). CT 1 month after procedure showed complete devascularization of the tumor (unenhanced CT **9a** and enhanced CT **9b**)

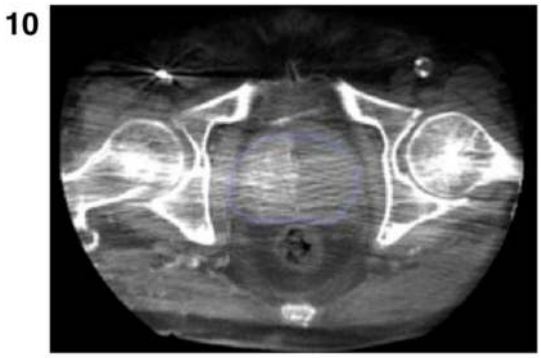

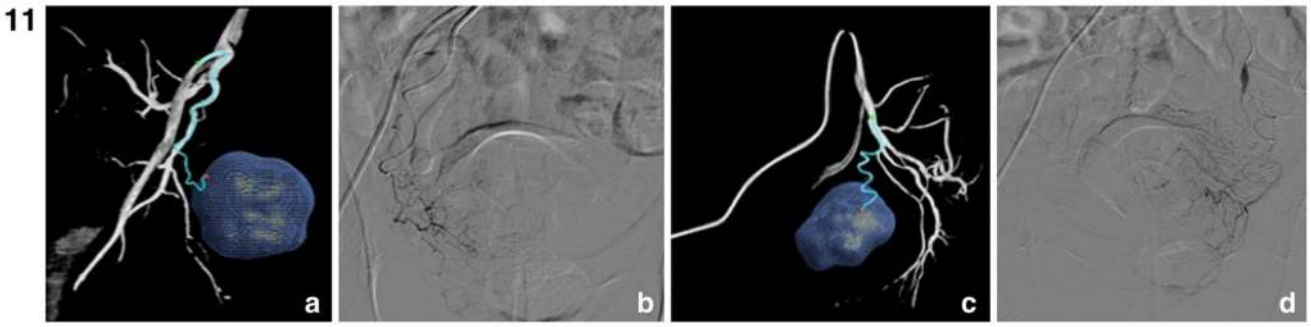

Figs. 10-11.

Prostate Embolization. Prostate enhancement on delayed phase where segmentation was performed (**10**). Emboguide software detected one right prostatic artery and one left PA (**11a, c**) which were seen on 2D arteriography (**11b, d**)

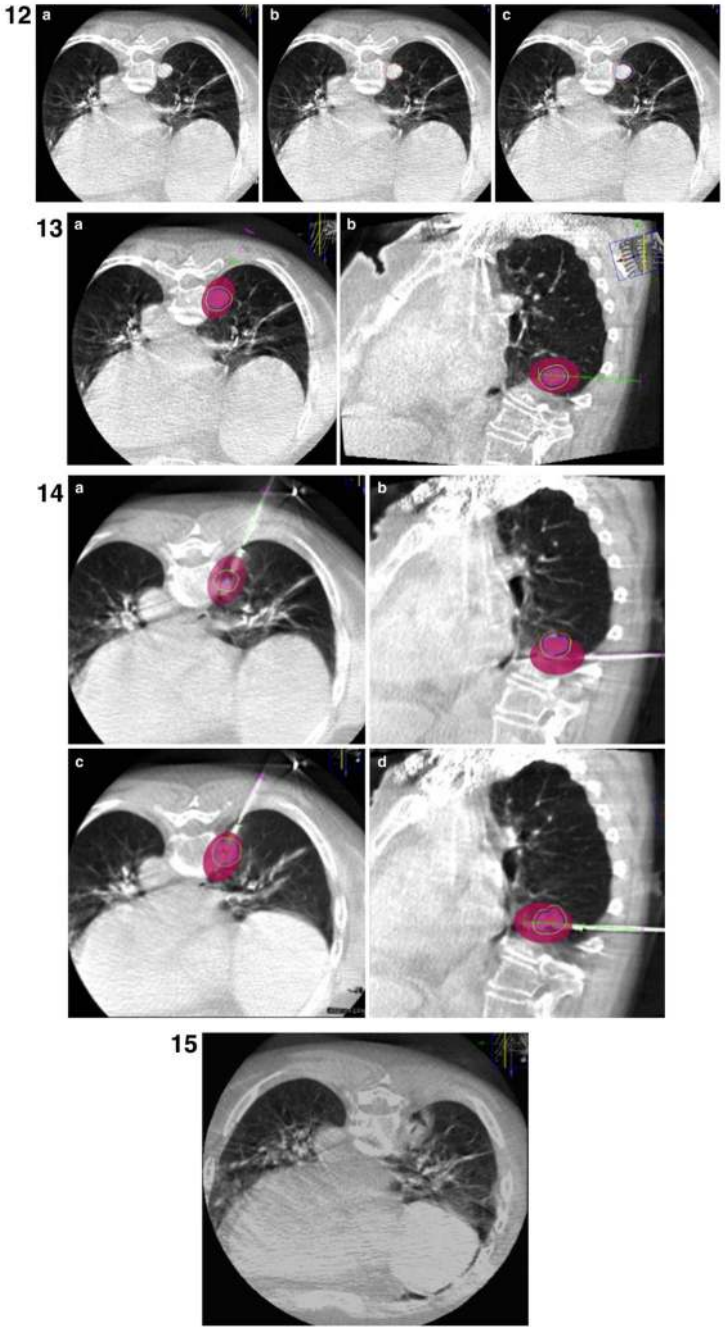

Figs. 12-15.

65-year-old male, Colon rectal cancer lung metastasis: MWA ablation. Fig. **12** Pre-procedural CBCT: lesion visualization (**12a**) with Lesion Segmentation (*orange line*) (**12b**) and adding 5 mm safe margins (*blue line lesion*; *orange line safe margins*) (**12c**). Fig. **13** Ablation planning: MW virtual probe with predicted ablation area (manufacturer specific) overlaying to segmented lesion with 5 mm safe margins covered in axial (**13a**) and progression view visualization (**13b**). Fig. **14** Intra-procedural CBCT: wrong MW probe placement (**14a, b**) with upper zone of lesion uncovered by the predictable ablation area

(**14b**); and subsequent repositioning with all lesion with 5 mm safe margins covered by the predictable ablation area. Fig. **15** Post-procedural CBCT, any complication demonstrated